

OPEN ACCESS

EDITED BY Giovanna Batoni, University of Pisa, Italy

REVIEWED BY
Manuel Espinosa-Urgel,
Spanish National Research Council (CSIC),
Spain
Wenxiu Zhu,
Shenyang Normal University, China

*CORRESPONDENCE
Renfei Lu

☑ rainman78@163.com
Yiquan Zhang
☑ zhangyiquanq@163.com

[†]These authors have contributed equally to this work and share first authorship

RECEIVED 25 June 2025 ACCEPTED 11 August 2025 PUBLISHED 20 August 2025

CITATION

Ni B, Chang J, Zhou Y, Li W, Tian Z, Lu R and Zhang Y (2025) The coordinated regulatory impact of AcsS and TpdA on biofilm formation in *Vibrio parahaemolyticus*. *Front. Microbiol.* 16:1652011. doi: 10.3389/fmicb.2025.1652011

COPYRIGHT

© 2025 Ni, Chang, Zhou, Li, Tian, Lu and Zhang. This is an open-access article distributed under the terms of the Creative Commons Attribution License (CC BY). The use, distribution or reproduction in other forums is permitted, provided the original author(s) and the copyright owner(s) are credited and that the original publication in this journal is cited, in accordance with accepted academic practice. No use, distribution or reproduction is permitted which does not comply with these terms.

The coordinated regulatory impact of AcsS and TpdA on biofilm formation in *Vibrio* parahaemolyticus

Bin Ni^{1†}, Jingyang Chang^{2†}, Yining Zhou^{1,3}, Wanpeng Li^{1,4}, Zhukang Tian^{1,4}, Renfei Lu^{3*} and Yiguan Zhang^{3*}

¹Department of Laboratory Medicine, School of Medicine, Jiangsu University, Zhenjiang, China, ²Department of Clinical Laboratory, Children's Hospital of Soochow University, Suzhou, China, ³Department of Clinical Laboratory, Nantong Third People's Hospital, Affiliated Nantong Hospital 3 of Nantong University, Nantong, China, ⁴Health Commission of Qinghai Province, Xining, China

Vibrio parahaemolyticus, a marine pathogen, employs biofilm formation to enhance environmental persistence and transmission. Biofilm development is intricately regulated by cyclic di-GMP (c-di-GMP), whose levels are controlled by diguanylate cyclases (DGCs) and phosphodiesterases (PDEs). This study elucidates the coordinated regulatory roles of the LysR-type transcriptional regulator AcsS and the PDE TpdA in biofilm formation. Through genetic, transcriptomic, and biochemical analyses, we demonstrate that AcsS promotes biofilm formation by directly activating the exopolysaccharide biosynthesis gene cpsA and indirectly repressing tpdA, a gene encoding a c-di-GMP-degrading enzyme. Conversely, TpdA inhibits acsS expression and antagonizes cpsA transcription. RNA-seq revealed that AcsS globally regulates 235 genes, including those linked to flagella, type IV pili, and capsular polysaccharides. Intracellular c-di-GMP quantification showed that AcsS elevates c-di-GMP levels, while TpdA reduces them, establishing a feedback loop. Phenotypic assays confirmed that AcsS-dependent biofilm enhancement operates independently of TpdA, though TpdA partially suppresses biofilm formation in the absence of AcsS. These findings unveil a regulatory circuit where AcsS and TpdA coordinately modulate c-di-GMP metabolism and biofilm-associated gene expression, highlighting them as promising targets for disrupting biofilm-mediated persistence and transmission of V. parahaemolyticus.

KEYWORDS

Vibrio parahaemolyticus, biofilm, AcsS, regulation, TpdA, c-di-GMP

Introduction

Vibrio parahaemolyticus (V. parahaemolyticus) is a bacterium that thrives in marine ecosystems (Baker-Austin et al., 2018). It poses a health risk primarily through the consumption of contaminated seafood, and to a lesser extent, via contact with seawater through small open wounds (Baker-Austin et al., 2018). Additionally, this bacterium is capable of forming biofilms on a range of surfaces, including those found on seafood products (Sharan et al., 2022). Biofilms are bacterial communities encased in a matrix that forms on surfaces and are widely utilized by numerous bacterial species to enhance environmental fitness and facilitate transmission (Yildiz and Visick, 2009; Faruque et al., 2006). The biofilm matrix, which constitutes over 90% of the mass of a biofilm, is predominantly composed of exopolysaccharides (EPS), extracellular proteins, extracellular DNA, and lipids, with EPS being a particularly significant component (Flemming and

Wingender, 2010). In *V. parahaemolyticus*, the production of EPS is linked to the *cpsA-K* (VPA1403-1413) and *scvA-O* operons (Liu et al., 2022). Deletion of either operon leads to a decrease in biofilm formation (Liu et al., 2022). Specifically, the *cpsA-K* operon, rather than the *scvA-O* operon, is directly correlated with the transition between wrinkled and smooth colony morphologies in *V. parahaemolyticus*, with the wrinkled variant associated with increased EPS production (Liu et al., 2022). Furthermore, additional structures, including flagella and type IV pili, also influence the biofilm formation of *V. parahaemolyticus* (Yildiz and Visick, 2009).

Biofilm formation is tightly regulated by numerous factors, with the secondary messenger cyclic dimeric GMP (c-di-GMP) being of central relevance. Elevated levels of c-di-GMP typically enhance biofilm formation while simultaneously suppressing motility (Yildiz and Visick, 2009). The synthesis of c-di-GMP is facilitated by the GGDEF domain present in diguanylate cyclases (DGCs), while its degradation is mediated by the EAL or HD-GYP domain found in phosphodiesterases (PDEs) (Jenal et al., 2017). In V. parahaemolyticus, proteins with both GGDEF and EAL domains, such as ScrC and ScrG, as well as those with only the EAL domain, like LafV and TpdA, have been shown to serve as PDEs that inhibit biofilm formation and/or promote motility (Boles and McCarter, 2002; Kim and McCarter, 2007; Kimbrough and McCarter, 2021; Martínez-Méndez et al., 2021). Furthermore, proteins harboring the GGDEF domain, including ScrM, ScrJ, ScrL, and GefA, have been identified as DGCs that either promote biofilm formation or inhibit motility (Kimbrough and McCarter, 2021; Kimbrough et al., 2020; Zhong et al., 2022). Additionally, VopY, an EAL domain-containing protein, degrades c-di-GMP, thereby augmenting virulence (Wu et al., 2023). The metabolism of c-di-GMP is intricately regulated by various environmental conditions, including salinity, exposure to antibiotics like chloramphenicol, and the availability of nutrients such as L-arabinose (Li et al., 2021; Zhang et al., 2023; Zhang et al., 2023). Moreover, transcriptional regulators such as OpaR, QsvR, and H-NS modulate c-di-GMP metabolism by regulating the expression of genes encoding DGCs and PDEs (Zhang et al., 2021; Xue et al., 2022; Zhang et al., 2023).

AcsS, a member of LysR-family transcriptional regulators, is significantly regulated by environmental factors, including low-salt growth conditions, the presence of L-arabinose, and incubation time (Zhang et al., 2023; Yang et al., 2010; Zhang et al., 2023). Our recent findings indicate that AcsS enhances the swimming and swarming motility of V. parahaemolyticus by activating the expression of genes associated with polar and lateral flagella (Chang et al., 2024), but it inhibits the expression of major virulence determinants, such as thermostable direct hemolysin and type VI secretion system 2, by repressing the transcription of corresponding genes (Ni et al., 2025; Ni et al., 2024). Notably, flagella play a crucial role in the initial stages of biofilm formation and are essential for the development of mature biofilms in V. parahaemolyticus (Yildiz and Visick, 2009; Enos-Berlage et al., 2005). Therefore, AcsS is likely involved in regulating biofilm formation in V. parahaemolyticus. In this study, our data demonstrate that AcsS coordinates with TpdA to regulate biofilm formation in V. parahaemolyticus.

Materials and methods

Bacterial strains

The wild type (WT) strain RIMD2210633 of *V. parahaemolyticus* was utilized in this study (Makino et al., 2003). Nonpolar *acsS* deletion mutant ($\Delta acsS$), derived from the WT strain, was constructed by our previous study (Chang et al., 2024). The complementation strain $\Delta acsS$ / pBAD33-*acsS* (C- $\Delta acsS$) was constructed by introducing pBAD33-*acsS* into $\Delta acsS$ (Chang et al., 2024). Control strains (WT/pBAD33 and $\Delta acsS$ /pBAD33) were generated by introducing pBAD33 into WT and $\Delta acsS$, respectively. The *acsS* and *tpdA* double-gene mutant ($\Delta acsS\Delta tpdA$) and the *tpdA* single-gene mutant ($\Delta tpdA$) were generated via deletion of a 258-bp fragment (nucleotides 1305–1562) of *tpdA* from $\Delta acsS$ and WT, respectively, by homologous recombination using suicide plasmid pDS132 (Sun et al., 2012). All primers used in this study are listed in Table 1.

Growth conditions

Unless stated otherwise, the cultivation of *V. parahaemolyticus* was conducted as previously described (Lu et al., 2021). Briefly, *V. parahaemolyticus* was grown in 2.5% (w/v) Bacto heart infusion (HI) broth (BD Biosciences, New Jersey, United States) at 37 °C with shaking at 200 rpm for 12 h. The resultant culture was diluted 50-fold into 5 mL HI broth, and then incubated under the same conditions until it reached to an optical density at 600 nm (OD $_{600}$) value of 1.4. This culture was referred to as the bacterial seed. Subsequently, the bacterial seed was diluted 1,000-fold into 5 mL of HI broth for a third round of growth and was harvested at an OD $_{600}$ value of 1.4. When necessary, the medium was supplemented with 50 µg/mL of gentamicin, 5 µg/mL of chloramphenicol and/or 0.1% (w/v) L-arabinose.

Crystal violet staining assay

Crystal violet (CV) staining assay was performed similarly as previously described (Zhang et al., 2023). Briefly, the bacterial seed was diluted 50-fold into 2 mL of Difco marine (M) broth 2216 (BD Biosciences, New Jersey, United States), supplemented 5 µg/mL chloramphenicol and 0.1% L-arabinose, in a 24-well cell culture plate, and then incubated at 30 °C with shaking at 150 rpm for 24 h. Planktonic cells were collected for measurement of OD $_{600}$ values. Surface attached biofilm cells were washed with deionized water, and then stained by 0.1% CV. Bound CV was dissolved in 2.5 mL of 20% acetic acid, and then the OD $_{570}$ values were measured. The capacity for biofilm formation was expressed as the ratio of OD $_{570}$ to OD $_{600}$.

Colony morphology assay

For the colony morphology assay (Zhang et al., 2023), the overnight bacterial culture was diluted 50-fold into 5 mL M broth, and it was then statically incubated at 30 $^{\circ}$ C for 48 h. After thorough mixing, 2 μ L of the culture was spotted onto an HI plate, or an HI plate

TABLE 1 Primers used in this study.

Target	Primers (forward/reverse, 5'-3')	References	
Construction of m	nutant		
acsS	GTGACTGCAGTTCCACTGACGGTCATCAC/	Chang et al. (2024)	
	CGATAGGGATAATGCGAAGGGTCTGTTCAAGTGCGATG		
	CATCGCACTTGAACAGACCCTTCGCATTATCCCTATCG/		
	GTGAGCATGCGTTGTGCCAGCAAGATTTC		
	GTGACTGCAGTTCCACTGACGGTCATCAC/		
	GTGAGCATGCGTTGTGCCAGCAAGATTTC		
tpdA	GTGACTGCAGACACCAACACAGGTACATCG/	This study	
	GACGCAGCGTTTCCACTTTCCCTCGTAGAAGAGAAGGGCA		
	TGCCCTTCTCTACGAGGGAAAGTGGAAACGCTGCGTC/		
	GTGAGCATGCTGGTAAGCCTGTTCAAACGG		
	GTGACTGCAGACACCAACACAGGTACATCG/		
	GTGAGCATGCTGGTAAGCCTGTTCAAACGG		
Construction of co	omplementation strain		
acsS	GATTCTAGAAGGAGGAATTCACCATGGATATCAAACAAC/	Chang et al. (2024)	
	GTGACTGCAGTTATCGATTAAATATG		
RT-qPCR			
cpsA	GAGAGCGGCAACCTATATCG/CGCCACGCCAACAGTAATG	Zhang et al. (2023)	
tpdA	AGAATCAACCAACACACACAAATACTGTTGATGGCGTA	This study	
LacZ fusion			
cpsA	GCGCGAGCTCCTTCCCTGTAAATAAGTCATCC/	Zhang et al. (2023)	
	GCGCGGATCCAAGCGAACTCCATCTCATAAG		
tpdA	TCGATAAGCCCGAGTGAAT/TGAGTATGCCATTCTTTCAAC	This study	
Two-plasmid Lac	Z fusion		
cpsA	GCGCGAGCTCCTTCCCTGTAAATAAGTCATCC/	Zhang et al. (2023)	
	GCGCGGATCCAAGCGAACTCCATCTCATAAG		
tpdA	TCGATAAGCCCGAGTGAAT/TGAGTATGCCATTCTTTCAAC	This study	
EMSA			
cpsA	GCGCGTCGACCTTCCCTGTAAATAAGTCATCC/	Zhang et al. (2023)	
	GCGCGAATTCAAGCGAACTCCATCTCATAAG		
tpdA	TCGATAAGCCCGAGTGAAT/TGAGTATGCCATTCTTTCAAC	This study	
16S rRNA	GACACGGTCCAGACTCCTAC/GGTGCTTCTTCTGTCGCTAAC	Zhang et al. (2023)	

supplemented with $5\,\mu g/mL$ chloramphenicol and 0.1% (w/v) L-arabinose, and incubated at 37 $^{\circ}C$ for 48 h.

RNA isolation and RNA sequencing

The WT and $\Delta acsS$ strains were incubated under the same conditions as the CV staining assay, but without the addition of chloramphenicol and L-arabinose. Three technical replicates were conducted for each strain. Bacterial cells were harvested simultaneously from biofilms and planktonic fractions for the preparation of total RNA, which was extracted using TRIzol Reagent (Invitrogen, Massachusetts, United States) (Zhang et al., 2023). One RNA sample was prepared from each technical replicate. RNA concentration and integrity were determined by a Nanodrop 2000 and the agarose gel electrophoresis, respectively. rRNA removal and mRNA enrichment were performed using an Illumina/Ribo-ZeroTM rRNA Removal Kit

(bacteria) (Illumina, California, United States). All RNA-related manipulations including RNA extraction were performed in GENEWIZ Biotechnology Co. Ltd. (Suzhou, China). cDNA sequencing was performed on an Illumina Hiseq platform (Zhang et al., 2023; Zhang et al., 2022). Gene expression in $\Delta acsS$ (test group) was compared with that in WT (reference group). DESeq (v1.12.4) was used to identify the differentially expressed genes (DEGs), filtering for $p \leq 0.01$ and absolute FoldChange ≥ 2 . DEGs were further analyzed using the Gene Ontology (GO), Kyoto Encyclopedia of Genes and Genomes (KEGG) pathway, and Cluster of Orthologous Groups of proteins (COG) database (Zhang et al., 2023; Zhang et al., 2022).

Intracellular c-di-GMP quantification

Intracellular c-di-GMP was quantified as previously described (Zhang et al., 2023). Briefly, bacterial cells were harvested at an OD_{600}

value of 1.4, and then they were resuspended in 2 mL ice-cold phosphate buffered saline (PBS). The bacterial suspension was incubated at 100 °C for 5 min, sonicated for 15 min, and then centrifuged at 9,000 g for 5 min. Total protein and c-di-GMP levels in the supernatant were determined using a Pierce BCA Protein Assay kit (ThermoFisher Scientific, Massachusetts, United States) and a c-di-GMP Enzyme-linked Immunosorbent Assay (ELISA) Kit (Mskbio, Hubei, China), respectively. The c-di-GMP level was expressed as pmol/g of protein.

Real-time quantitative PCR

Bacterial cells were harvested at an OD $_{600}$ value of 1.4. Total RNA was extracted using TRIzol Reagent (Invitrogen, Massachusetts, United States). cDNA was generated from 1 μ g of total RNA using a FastKing First Strand cDNA Synthesis Kit (Tiangen Biotech, Beijing, China). Real-time quantitative PCR (RT-qPCR) was performed using a LightCycler 480 (Roche, Basel, Switzerland) together with SYBR Green master mix (Tiangen Biotech, Beijing, China) (Gao et al., 2011). The relative expression levels of each target gene were determined using the $2^{-\Delta\Delta Ct}$ method, with the 16S rRNA serving as the internal control.

LacZ fusion and β-galactosidase assay

The regulatory DNA region of each target gene was cloned into pHRP309 harboring a promoterless lacZ gene and a gentamicin resistance gene (Parales and Harwood, 1993). Each recombinant plasmid was transferred into WT and its corresponding mutants. Transformants were cultured and lysed to measure the β-galactosidase activity of the cellular extracts using a β-Galactosidase Enzyme Assay System (Promega, Wisconsin, USA). Miller Units representing the β -galactosidase activity was calculated as previously described (Zhang et al., 2023). For the two-plasmid lacZ reporter assay (Zhang et al., 2023), the recombinant pHRP309 was transferred into Escherichia coli 100 λpir (EC100; Epicenter, Wisconsin, USA) bearing pBAD33-acsS or pBAD33. The transformants were cultured in Luria-Bertani (LB) broth containing 0.1% L-arabinose and 20 μg/mL chloramphenicol at 37 °C with shaking at 200 rpm. Bacterial cells were harvested at an OD_{600} value of 1.2, and then lysed to measure the β -galactosidase activity in the cell extracts.

Purification of 6 × His-AcsS and electrophoretic mobility-shift assay

The coding region of *acsS* was cloned into pET28a (Novagen, Darmstadt, Germany). The recombinant pET28a plasmid was transferred into *E. coli* BL21 λ DE3 to express the His-tagged AcsS protein (His-AcsS). Expression and purification of His-AcsS were performed as previously described for His-OpaR (Sun et al., 2012). The purity of His-AcsS was confirmed by sodium dodecyl sulfate-polyacrylamide gel electrophoresis. The concentration of His-AcsS solution was determined using a Pierce BCA Protein Assay kit. Purified His-AcsS was stored at $-60\,^{\circ}$ C.

For electrophoretic mobility-shift assay (EMSA) (Zhang et al., 2023), the regulatory DNA region of each target gene was amplified by PCR. EMSA was performed in a 10 μL reaction volume containing 0.5 mM EDTA, 1 mM MgCl $_2$, 50 mM NaCl, 0.5 mM DTT, 10 mM Tris–HCl (pH 7.5), 0.625 $\mu g/mL$ salmon sperm DNA, 100 ng target DNA, and a certain amount of His-AcsS. After incubation at room temperature for 20 min, the binding reactions were visualized on a native polyacrylamide gel, which was stained with ethidium bromide and analyzed using a UV transilluminator.

Replicates and statistical methods

The CV staining, colony morphology assay, c-di-GMP measurement, LacZ fusion assay, RT-qPCR, and two-plasmid lacZ fusion assay were performed at least three times, with at least three technical replicates each time. EMSA for each target gene was performed at least two times, independently. The numerical results were expressed as the mean \pm standard deviation (SD). To calculate statistical significance, Student's t-tests or two-way ANOVA with Tukey's $post\ hoc$ corrections were applied, considering a p value of less than 0.05 as significant.

Results

AcsS promotes biofilm formation by Vibrio parahaemolyticus

AcsS is involved in promoting the swimming and swarming motility of *V. parahaemolyticus*, which are required for mature biofilm formation (Chang et al., 2024; Enos-Berlage et al., 2005). We therefore investigated the potential regulatory role of AcsS in biofilm formation by *V. parahaemolyticus*. As depicted in Figure 1a, the $\Delta acsS/pBAD33$ strain displayed remarkably reduced CV staining compared to both the WT/pBAD33 and C- $\Delta acsS$ strains (p < 0.01). Notably, the C- $\Delta acsS$ strain demonstrated a restored CV staining pattern indicative of biofilm formation. Additionally, the colony of $\Delta acsS$ appeared smoother than that of WT (Figure 1b). Moreover, the colonies of both WT/pBAD33 and C- $\Delta acsS$ appeared smoother than that of WT. This observation may

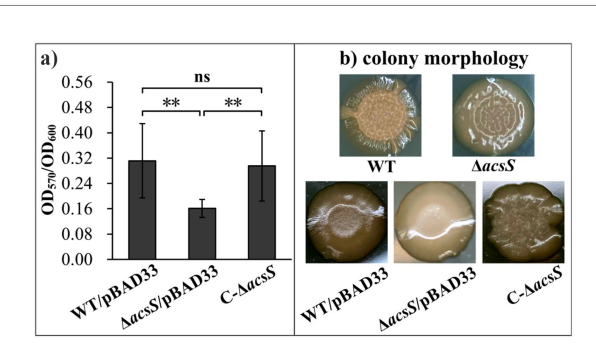


FIGURE 1
AcsS activates biofilm formation by *V. parahaemolyticus*. Biofilm formation by *V. parahaemolyticus* was assessed using crystal violet staining (a) and colony morphology (b). Photographs represent three independent experiments, each with at least three replicates. Twoway ANOVA with Tukey's *post hoc* corrections were utilized to determine statistical significance. **p < 0.01.

be attributed to the significant influence of chloramphenicol and L-arabinose on this particular phenotype (Zhang et al., 2023; Zhang et al., 2023). While the colony morphology of C-ΔacsS and WT/pBAD33 appeared quite different, both exhibited a more wrinkled appearance compared to ΔacsS/pBAD33. Since mutation of acsS does not affect the growth of *V. parahaemolyticus* (Chang et al., 2024), these results indicate that AcsS positively regulates biofilm formation in *V. parahaemolyticus*.

Screening for potential target genes of AcsS involved in biofilm formation using RNA-seq

To determine the regulatory mechanism of AcsS on biofilm formation in V. parahaemolyticus, RNA sequencing (RNA-seq) analysis was performed comparing the $\triangle acsS$ (test) and WT (reference) strains. As shown in Figure 2a and detailed in Supplementary Table S1, 235 genes were identified as regulated by AcsS under biofilm growth conditions. Of these, 78 genes were upregulated and 157 genes were downregulated, in $\Delta acsS$ compared to WT. GO term enrichment analysis indicated that DEGs were associated with molecular functions (7 GO terms, 29 DEGs), cellular components (5 GO terms, 42 DEGs) and biological processes (13 GO terms, 41 DEGs) (Figure 2b). KEGG pathway enrichment results revealed that 181 DEGs mapped to pathways including metabolism, human diseases, genetic information processing, environmental information processing, and cellular processes (Figure 2c). COG enrichment analysis categorized DEGs into 19 functional groups, with the most significant enrichment in function unknown and metabolismrelated categories (Figure 2d). These findings suggested that AcsS regulates global gene expression in V. parahaemolyticus.

As listed in Table 2, several DEGs implicated in biofilm formation were identified, including *tpdA*, *flgD*, *flgE*, *motY*, *mshG*, *capF*, and VP0226. Specifically, *tpdA* encodes a trigger PDE involved in biofilm formation and c-di-GMP degradation (Martínez-Méndez et al., 2021). The genes *flgD*, *flgE*, and *motY* are associated with the polar flagellar system, while *mshG* belongs to the type IV pili gene cluster. Additionally, *capF* and VP0226 contribute to capsular polysaccharide (CPS) synthesis. However, AcsS is unlikely to promote biofilm formation solely through polar flagella, type IV pili, and CPS, given the extensive gene networks governing these structures in *V. parahaemolyticus* (Makino et al., 2003). The *cpsA-K* gene cluster, directly associated with the wrinkled colony phenotype and regulated by TpdA (Liu et al., 2022), further underscores this complexity. Consequently, *tpdA* and *cpsA* (VPA1403) were selected as focal genes for subsequent experiments.

Regulation of *tpdA* and *cpsA* by AcsS and TpdA

The RT-qPCR results showed that the mRNA level of tpdA significantly increased in $\Delta acsS$ and $\Delta acsS\Delta tpdA$ but decreased in $\Delta tpdA$ compared to WT (Figure 3a). Specifically, tpdA mRNA levels were significantly lower in $\Delta acsS\Delta tpdA$ than in $\Delta acsS$ and significantly higher than in $\Delta tpdA$ (p < 0.05) (Figure 3a). Furthermore, the mRNA level of cpsA significantly decreased in $\Delta acsS$ and increased in $\Delta tpdA$, whereas no significant change was observed in $\Delta acsS\Delta tpdA$ compared to WT (Figure 3a). Compared to $\Delta tpdA$, the cpsA mRNA level was significantly elevated in $\Delta acsS\Delta tpdA$ but significantly reduced relative to $\Delta acsS$ (p < 0.05) (Figure 3a). As further determined by LacZ fusion assay

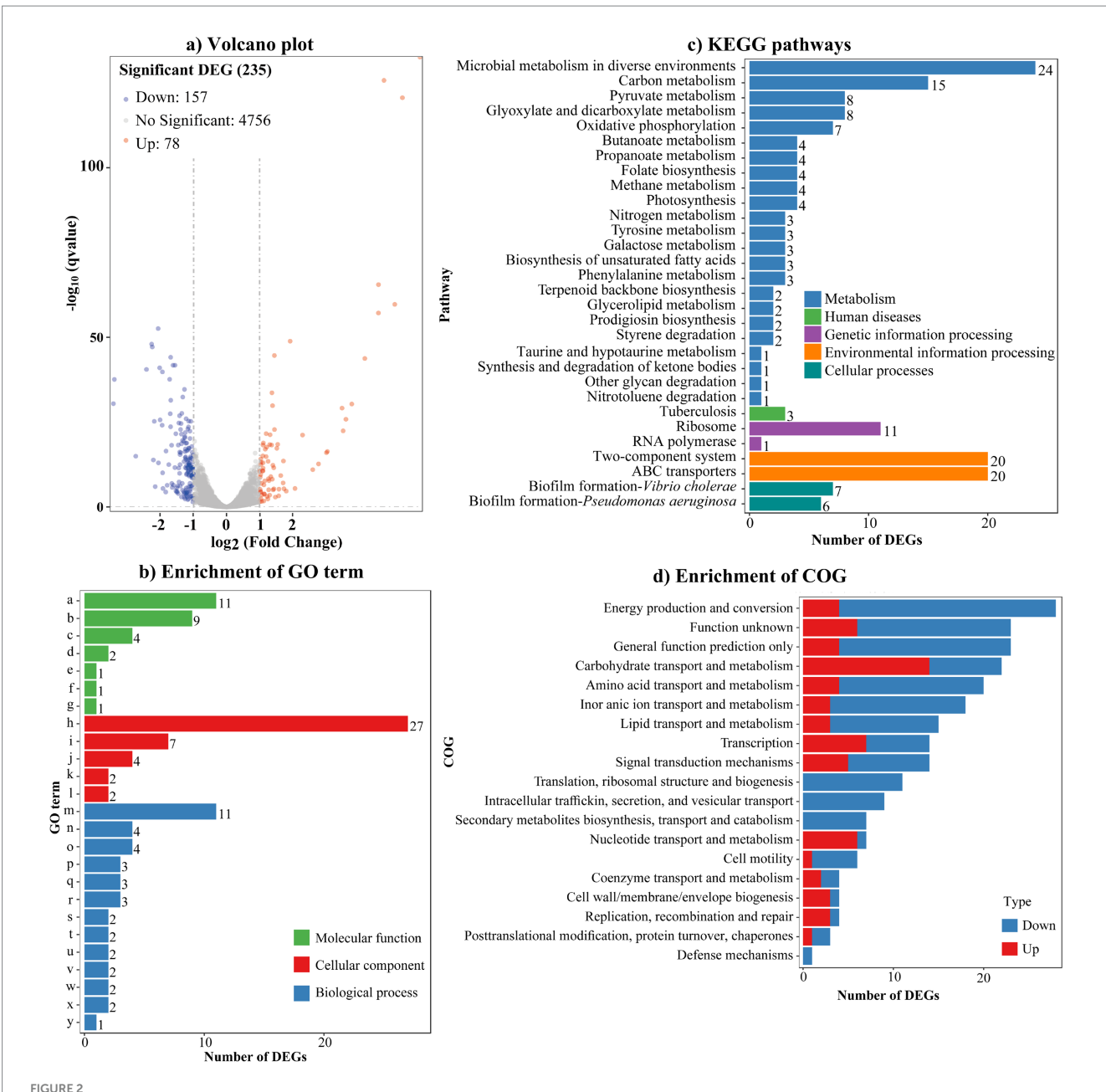
(Figure 3b), the promoter activity of tpdA significantly increased in $\Delta acsS$ and $\Delta acsS\Delta tpdA$ but significantly decreased in $\Delta tpdA$ compared to WT (p < 0.01). Additionally, the promoter activity of tpdA was significantly lower in $\Delta acsS\Delta tpdA$ than in $\Delta acsS$ and higher than in $\Delta tpdA$ (p < 0.01) (Figure 3b). For *cpsA*, promoter activity significantly decreased in $\Delta acsS$ and $\triangle acsS\Delta tpdA$ but increased in $\triangle tpdA$ compared to WT (p < 0.01). Notably, cpsA promoter activity in $\triangle acsS\Delta tpdA$ was elevated relative to $\triangle acsS$ but reduced compared to $\triangle tpdA$ (p < 0.01) (Figure 3b). Both assays demonstrated that tpdA expression in $\Delta acsS\Delta tpdA$ exceeds WT levels, suggesting that AcsS's negative regulatory effect on tpdA outweighs TpdA's positive regulation. Regarding cpsA expression, a discrepancy was observed between the RT-qPCR and LacZ fusion results: RT-qPCR revealed no significant difference in cpsA mRNA levels between ∆acsS∆tpdA and WT, whereas LacZ assays showed significantly lower cpsA promoter activity in $\triangle acsS\Delta tpdA$ than in WT. This inconsistency warrants consideration. Possible explanations include: (Baker-Austin et al., 2018) the lacZ fusion construct might lack regulatory elements present in the native chromosomal context that modulate mRNA stability or post-transcriptional processing, leading to a discrepancy between promoter activity measured by the reporter and steady-state mRNA levels; or (Sharan et al., 2022) post-transcriptional regulatory mechanism (e.g., affecting mRNA stability or translation efficiency) could differentially influence the endogenous cpsA mRNA measured by RT-qPCR versus the heterologous *lacZ* mRNA transcribed from the *cpsA* promoter fusion. Collectively, despite this discrepancy for cpsA in the double mutant, the results consistently indicate that AcsS suppresses tpdA expression but activates cpsA, independent of TpdA. Conversely, TpdA promotes its own expression while repressing cpsA, regardless of AcsS.

AcsS indirectly represses *tpdA* transcription but directly activates *cpsA* transcription

The results of EMSA showed that His-AcsS dose-dependently binds to the regulatory DNA fragment of *cpsA* but does not bind to the regulatory DNA region of *tpdA* or the coding region of 16S rRNA (used as a negative control) (Figure 4a). Additionally, a two-plasmid *lacZ* reporter assay demonstrated that expressing *acsS* from pBAD33-*acsS* in EC100 significantly decreased *tpdA* promoter activity while increasing *cpsA* promoter activity (Figure 4b). Although the two-plasmid *lacZ* fusion assay is a widely used method to validate direct regulatory interactions (Zhang et al., 2021; Ante et al., 2015; Bina et al., 2016), results obtained in heterologous hosts like EC100 must be interpreted cautiously. Potential confounding factors include regulator overexpression and incompatibility or unintended interactions between the regulator and the host's cellular machinery. Collectively, these findings confirm that AcsS directly activates the transcription of *cpsA* and indirectly represses *tpdA* transcription.

AcsS promotes c-di-GMP production whereas TpdA degrades c-di-GMP in *Vibrio* parahaemolyticus

A previous study demonstrated that deletion of tpdA led to a 33% increase in c-di-GMP levels compared to WT during exponential growth (Martínez-Méndez et al., 2021). The data from this study also showed that the c-di-GMP level in $\Delta tpdA$ was significantly higher than in WT (p < 0.05) (Figure 5). Additionally, the c-di-GMP levels in $\Delta acsS$ were significantly reduced compared



AcsS controls the expression of global genes. (a) Volcano plot. Orange, blue and gray points represent the upregulated, downregulated and no-differential expressed genes in ΔacsS relative to WT, respectively. (b) Enrichment of gene ontology (GO) term. Letters from a-y on the Y axis indicate structural constituent of ribosome, rRNA binding, proton-transporting ATP synthase activity/rotational mechanism, transporter activity, 5-(carboxyamino) imidazole ribonucleotide mutase activity, molybdopterin synthase activity, methylglyoxal synthase activity, plasma membrane, ribosome, proton-transporting ATP synthase complex/catalytic core F (1), small ribosomal subunit, large ribosomal subunit, translation, oxidation-reduction process, "de novo" IMP biosynthetic process, carbohydrate transport, ATP synthesis coupled proton transport, phosphate ion transport, valine catabolic process, glyoxylate cycle, lipid catabolic process, L-phenylalanine catabolic process, poly-hydroxybutyrate biosynthetic process, D-gluconate metabolic process, and methylglyoxal biosynthetic process, respectively. (c) Enrichment of kyoto encyclopedia of genes and genomes (KEGG). (d) Enrichment of cluster of orthologous groups of proteins (COG). The number on the top of each bar in b and c indicates the number of DEGs.

to WT, $\Delta tpdA$ and $\Delta acsS\Delta tpdA$ (p < 0.05) (Figure 3). Furthermore, the c-di-GMP level in $\Delta acsS\Delta tpdA$ was significantly lower than that in $\Delta tpdA$ (p < 0.05) (Figure 3). However, no significant differences were detected when comparing $\Delta acsS\Delta tpdA$ with WT (p > 0.05) (Figure 5). These findings indicate that TpdA degrades c-di-GMP in V. parahaemolyticus independently of AcsS, while AcsS stimulates c-di-GMP synthesis regardless of TpdA's presence.

AcsS-dependent biofilm formation is independent of TpdA

To determine whether AcsS-dependent biofilm formation is mediated by TpdA, we compared the biofilm-forming abilities of the WT, $\Delta acsS$, $\Delta tpdA$ and $\Delta acsS\Delta tpdA$ strains. As depicted in Figure 6a, the $\Delta acsS$ and $\Delta acsS\Delta tpdA$ strains displayed significantly

TABLE 2 Selected DEGs.

Gene ID	Name	Fold change	Product	
c-di-GMP metabolism				
VP1881	tpdA	5.84	EAL domain protein	
Cell motility				
VP0777	flgD	0.48	Flagellar basal body rod modification protein	
VP0778	flgE	0.50	Flagellar hook protein FlgE	
VPA1539	motY	2.19	Sodium-type flagellar protein MotY	
Type IV pili				
VP2700	mshG	0.48	MSHA biogenesis protein MshG	
Capsule polysaccharide (CPS)				
VP0225	capF	0.44	Capsular polysaccharide biosynthesis protein	
VP0226		0.45	Rhamnosyl transferase	
Regulatory functions				
VP0080		2.00	Sigma-54 interacting response regulator	
VP0350	calR	3.99	Leucine transcriptional activator	
VP0358		2.04	DeoR family transcriptional regulator	
VP0569	phoB	0.33	DNA-binding response regulator PhoB	
VP0570	phoR	0.29	Phosphate regulon sensor protein	
VP1244		0.49	Response regulator	
VP2387		2.02	DeoR family transcriptional regulator	
VP2885	fis	0.44	DNA-binding protein Fis	
VPA0148	cpxR	0.43	Transcriptional regulator CpxR	
VPA0149	cpxA	0.47	Two-component system sensor kinase	
VPA0249		0.39	Transcriptional activator	
VPA0251		2.11	LysR family transcriptional regulator	
VPA0355		0.32	Transcriptional regulator	
VPA1472		2.14	MerR family transcriptional regulator	

reduced CV staining compared to the WT and $\Delta tpdA$ strains, respectively (p < 0.05). In contrast, the $\Delta acsS\Delta tpdA$ strain exhibited significantly enhanced CV staining relative to the $\Delta acsS$ strain (p < 0.01). However, no significant difference was observed between the $\Delta tpdA$ and WT strains (p > 0.05). Additionally, the colonies of WT and $\Delta tpdA$ were more wrinkled than those of the $\Delta acsS$ and $\Delta acsS\Delta tpdA$ strains (Figure 6b). The colonies of $\Delta tpdA$ and $\Delta acsS\Delta tpdA$ were slightly wrinkled compared to those of the WT and $\Delta acsS$ strain, respectively (Figure 6b). These results suggest that AcsS-dependent biofilm formation is independent of TpdA, while TpdA appears to partially suppress biofilm formation in the $\Delta acsS$ genetic background.

TpdA inhibits the expression of acsS

To determine whether TpdA regulates *acsS*, we analyzed *acsS* mRNA levels by RT-qPCR. As shown in Figure 7, the mRNA levels of *acsS* were significantly elevated in the $\Delta tpdA$ strain compared to the WT strain (p < 0.01), suggesting that the expression of *acsS* was under the negative control of TpdA in *V. parahaemolyticus*.

Discussion

LysR-type transcriptional regulators are crucial for a wide range of cellular processes, including metabolism, motility, biofilm formation, and virulence, through their control of gene transcription (Mayo-Pérez et al., 2023). In this study, the data demonstrated that the LysR-type transcriptional regulator AcsS exerts a positive regulatory effect on biofilm formation in *V. parahaemolyticus* (Figure 1). Notably, the expression of AcsS is significantly induced by low-salt growth conditions and L-arabinose, both of which greatly affect biofilm formation in this pathogen (Zhang et al., 2023; Yang et al., 2010). Therefore, further research is necessary to ascertain whether the effects of salinity and L-arabinose on biofilm formation is mediated through the regulation of AcsS.

RNA-seq analysis revealed that AcsS controls 235 genes implicated in a variety of cellular pathways (Supplementary Table S1). However, only a subset of these genes is linked to biofilm formation, including three flagellar genes, one type IV pili-related gene, two CPS biosynthesis genes, and one gene linked to c-di-GMP metabolism (Table 2). Mature biofilm

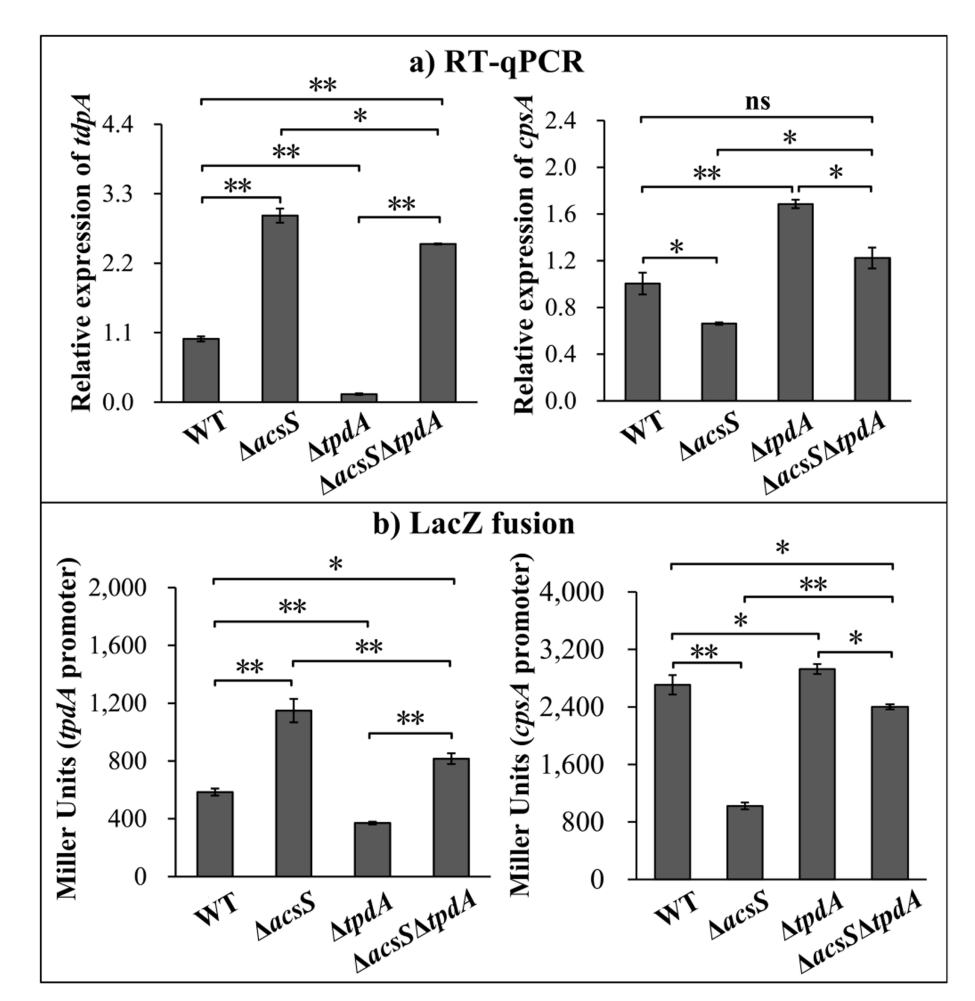


FIGURE 3
Regulation of tpdA and cpsA by AcsS and TpdA. V. parahaemolyticus strains were grown in HI broth, and bacterial cells were harvested at an OD₆₀₀ value of 1.4. Two-way ANOVA with Tukey's post hoc corrections were utilized to determine statistical significance. *p < 0.05. **p < 0.01. (a) RT-qPCR. The relative mRNA levels of each target gene were examined and compared between the WT, $\Delta acsS$, $\Delta tpdA$, and $\Delta acsS\Delta tpdA$ strains. (b) LacZ fusion. The regulatory DNA region of each target gene was cloned into pHRP309 and transferred into indicated strains. This was done to determine the β -galactosidase activities (Miller units) in the cellular extracts.

development requires polar and lateral flagella (Yildiz and Visick, 2009; Enos-Berlage et al., 2005). Type IV pili serve as adhesins that facilitate formation of biofilms on surfaces, particularly chitin (Shime-Hattori et al., 2006; Frischkorn et al., 2013). CPS plays a pivotal role in controlling biofilm size by limiting the expansion of mature biofilms (Lee et al., 2013). However, the synthesis of flagella, type IV pili, and CPS involves multiple genes (Makino et al., 2003). It remains unclear whether AcsS has a global impact on the overall synthesis of these structures under the tested conditions, as its regulatory effects appear limited to individual genes within these intricate systems. AcsS indirectly represses the transcription of tpdA, which encodes a PDE that degrades c-di-GMP, thereby inhibiting biofilm formation (Martínez-Méndez et al., 2021). In a feedback loop, TpdA inhibits the expression of both acsS and its own gene (Figures 3, 4, 7). AcsS-dependent c-di-GMP production may be mediated through TpdA, whereas TpdA inhibits c-di-GMP production independently of AcsS (Figure 5). Moreover, AcsS-dependent biofilm formation is not influenced by TpdA, although TpdA partially inhibits biofilm formation in the $\Delta acsS$ background (Figure 6). Consequently, AcsS and TpdA coordinately regulate c-di-GMP levels, implicating this signaling molecule as one mechanism through which AcsS controls biofilm formation.

Deletion of acsS alone ($\Delta acsS$) or in combination with acsS and tpdA ($\Delta acsS\Delta tpdA$) resulted in smoother colony morphology compared to WT (Figures 1, 6). This phenotype aligns with reduced EPS production (Chen et al., 2010). In V. parahaemolyticus, the cpsA-K and scvA-O gene clusters are responsible for the production of EPS (Liu et al., 2022). However, only the cps locus drives EPS phase variation, which mediates transitions between smooth and wrinkled colony morphologies (Liu et al., 2022; Zhang et al., 2022). This variation influences various behaviors of V. parahaemolyticus, including motility, biofilm formation, and virulence gene expression (Zhang et al., 2022; Wu et al., 2023). The data presented here showed that AcsS directly activates cpsA expression independently of AcsS (Figures 3, 4). This antagonistic

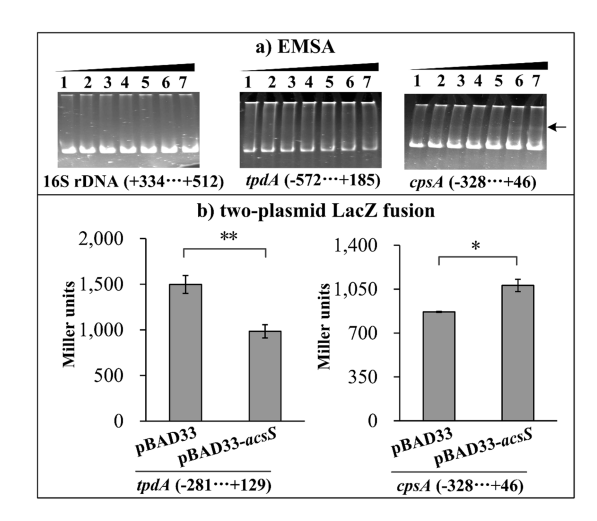


FIGURE 4

AcsS directly inhibits tpdA but indirectly regulates cpsA. Negative and positive numbers in brackets indicate the nucleotide positions upstream and downstream of each target gene, respectively. (a) EMSA. The regulatory DNA region of each target gene was incubated with increasing amounts of purified His-AcsS and then subjected to 6% (w/v) polyacrylamide gel electrophoresis. DNA bands were visualized using EB staining. Lanes 1 through 7 contain 0.0, 0.8, 1.6, 2.4, 3.2, 4.0, and 4.8 pmol of His-AcsS, respectively. The arrow indicates the shifted band. (b) Two-plasmid lacZ fusion assay. The plasmid pBAD33-acsS (or pBAD33) and a recombinant lacZ plasmid were simultaneously introduced into the E. coli strain 100 λpir (Epicenter). The promoter activities, measured in Miller units, of each target gene within the cellular extracts were determined using a β-Galactosidase Enzyme Assay System (Promega, United States) according to the manufacturer's instructions. Student's t-tests were utilized to determine statistical significance. **p < 0.01. ns, *p > 0.05.

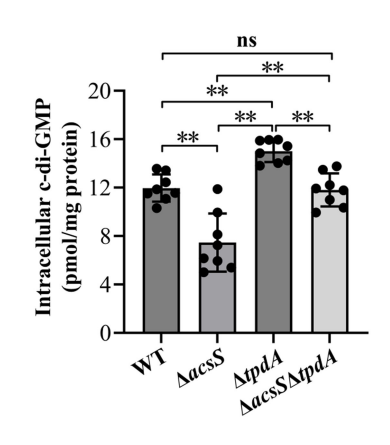
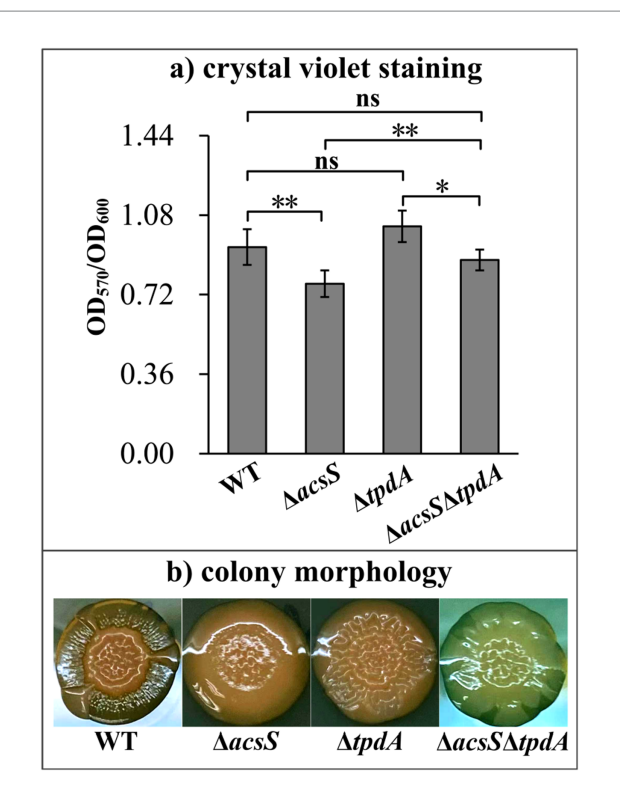


FIGURE 5

Intracellular c-di-GMP levels in different V. parahaemolyticus strains. V. parahaemolyticus strains were cultivated in HI broth, and bacterial cells were collected at an OD₆₀₀ value of 1.4. Intracellular c-di-GMP levels were measured using a c-di-GMP enzyme-linked immunosorbent assay (ELISA) kit. The results are presented as the means \pm SD from three independent experiments, with each experiment including at least three biological replicates. Two-way ANOVA with Tukey's $post\ hoc\ corrections\ were\ utilized\ to\ determine statistical significance. **p < 0.01. ns, <math>p$ > 0.05.

regulatory relationship suggests that AcsS-mediated control of the *cpsA-K* operon is a key mechanism underpinning its role in biofilm regulation.



IGURE 6

AcsS-dependent biofilm formation was independent of TpdA. The biofilm-forming capacities of the WT, $\Delta acsS$, $\Delta tpdA$, and $\Delta acsS\Delta tpdA$ strains were assessed using crystal violet staining (a) and colony morphology (b). Photographs represent three independent experiments, each with at least three replicates. Two-way ANOVA with Tukey's $post\ hoc$ corrections were utilized to determine statistical significance. *p < 0.05. **p < 0.01. ns, p > 0.05.

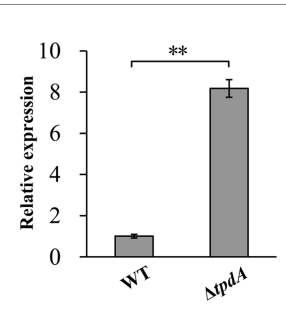
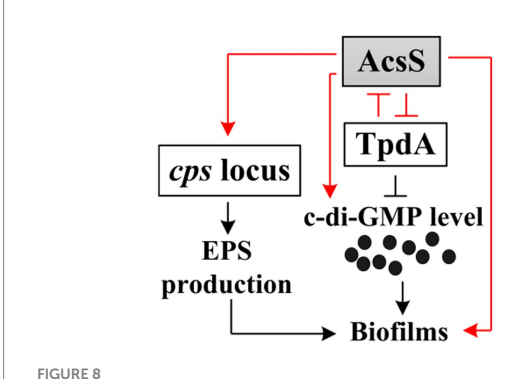


FIGURE 7

Regulation of acsS by TpdA. V. parahaemolyticus strains were grown in HI broth, and bacterial cells were harvested at an OD_{600} value of 1.4. The relative mRNA levels of each target gene were examined and compared between the WT and $\Delta tpdA$ strains. Student's t-tests were utilized to determine statistical significance. **p < 0.01.

Biofilm formation by *V. parahaemolyticus* is intricately controlled by a variety of factors, including nutritional conditions like salinity (Li et al., 2021), metal ion concentrations (Li et al., 2024; Li et al., 2024), and carbon sources (Zhang et al., 2023); environmental parameters like pH (Çam and Brinkmeyer, 2020) and temperature (Billaud et al., 2022); and regulatory proteins such as AphA (Chen et al., 2023), OpaR (Zhang et al., 2021), QsvR (Zhang et al., 2023), OxyR (Chung et al., 2016), CpsQ (Ferreira



Regulatory circuit. The arrows signify positive regulation, whereas the T-junctions denote negative regulation. The black dots indicate c-di-GMP. The regulatory relationships depicted by red lines are the findings of the current study, while those illustrated by black lines have been established in earlier research (Liu et al., 2022; Martínez-Méndez et al., 2021).

et al., 2012), ToxR (Chen et al., 2018), and H-NS (Zhang et al., 2018). QsvR directly represses the transcription of *aphA* and *toxR*, while activating cpsQ and opaR (Lu et al., 2021; Zhang et al., 2019). Furthermore, VPA0607 and qsvR are transcribed together as the VPA0607-qsvR operon (Zhang et al., 2023). AphA indirectly activates the transcription of VPA0607 at low cell density, whereas OpaR and QsvR directly repress it at high cell density (Zhang et al., 2023). This intricate interplay of regulators is particularly crucial for the precise control of biofilm-related gene expression. In this study, RNA-seq data revealed that AcsS regulates 12 putative regulatory genes, including calR, phoBR, and fis (Table 2). Among these, CalR regulates virulence (Zhang et al., 2017), swarming motility (Gode-Potratz et al., 2010), and biofilm formation (unpublished data). PhoB and PhoR form a two-component signal transduction system (Ortet et al., 2015). In V. cholerae, PhoB positively regulates motility and negatively controls biofilm formation and c-di-GMP production (Pratt et al., 2009). In V. parahaemolyticus, PhoR is involved in regulating the expression of 1,122 genes, including those responsible for lateral flagella (Zhang et al., 2020). V. parahaemolyticus Fis functions as a global regulator, influencing a variety of biological processes such as quorum sensing, the modulation of swimming and swarming motility, and metabolic pathways (Tague et al., 2021). These findings suggest that AcsS may interact with CalR, PhoB/PhoR, Fis, and other regulators to form a coordinated network governing biofilm development. Further studies are needed to dissect these potential interactions and their mechanistic roles.

In conclusion, this study demonstrates that AcsS and TpdA coordinately regulate biofilm formation in *V. parahaemolyticus* (Figure 8). AcsS indirectly represses the transcription of *tpdA*, which encodes a PDE that degrades c-di-GMP, thereby promoting the production of c-di-GMP. In a feedback loop, TpdA inhibits the expression of *acsS*. Additionally, AcsS directly activates the transcription of *cpsA* independently of TpdA, while TpdA antagonizes *cpsA* expression. Therefore, AcsS promotes biofilm formation in *V. parahaemolyticus* by regulating the transcription of *cpsA-K* and *tpdA*, as well as the production of c-di-GMP. The data enhance our understanding of the regulatory networks controlling biofilm formation in *V. parahaemolyticus* and highlight

AcsS as a key regulator of this process. Importantly, disrupting this regulatory circuit could attenuate biofilm formation, thereby reducing environmental persistence and seafood contamination by this pathogen. Future studies should explore small-molecule inhibitors targeting these regulators to validate their translational potential.

Data availability statement

The original data presented in the study are included in the article/Supplementary material. The raw data of RNA-seq have been deposited in the NCBI repository under accession number PRJNA913656.

Author contributions

BN: Formal analysis, Data curation, Investigation, Project administration, Resources, Writing – original draft. JC: Data curation, Formal analysis, Investigation, Writing – original draft. YinZ: Investigation, Writing – original draft. WL: Investigation, Resources, Writing – original draft. ZT: Investigation, Resources, Writing – original draft. RL: Funding acquisition, Project administration, Resources, Supervision, Validation, Writing – original draft. YiqZ: Conceptualization, Formal analysis, Methodology, Supervision, Validation, Visualization, Writing – review & editing.

Funding

The author(s) declare that financial support was received for the research and/or publication of this article. This work was supported by the National Key Research and Development Program of China (Grand No. 2023YFD1801302), the Nantong University Special Research Fund for Clinical Medicine (Grant No. 2022JZ010), and the Research and Development of the Etiology and Epidemic Prevention Technology System for Infectious Diseases on the Qinghai-Tibet Plateau (Grand No. 20220254). The funders had no role in the study design, data collection and analysis, decision to publish, or preparation of the manuscript.

Conflict of interest

The authors declare that the research was conducted in the absence of any commercial or financial relationships that could be construed as a potential conflict of interest.

Generative Al statement

The authors declare that no Gen AI was used in the creation of this manuscript.

Any alternative text (alt text) provided alongside figures in this article has been generated by Frontiers with the support of artificial intelligence and reasonable efforts have been made to ensure accuracy,

including review by the authors wherever possible. If you identify any issues, please contact us.

that may be evaluated in this article, or claim that may be made by its manufacturer, is not guaranteed or endorsed by the publisher.

Publisher's note

All claims expressed in this article are solely those of the authors and do not necessarily represent those of their affiliated organizations, or those of the publisher, the editors and the reviewers. Any product

Supplementary material

The Supplementary material for this article can be found online at: https://www.frontiersin.org/articles/10.3389/fmicb.2025.1652011/full#supplementary-material

References

Ante, V. M., Bina, X. R., Howard, M. F., Sayeed, S., Taylor, D. L., and Bina, J. E. (2015). *Vibrio cholerae* leuO transcription is positively regulated by ToxR and contributes to bile resistance. *J. Bacteriol.* 197, 3499–3510. doi: 10.1128/JB.00419-15

Baker-Austin, C., Oliver, J. D., Alam, M., Ali, A., Waldor, M. K., Qadri, F., et al. (2018). *Vibrio* spp. infections. *Nat. Rev. Dis. Primers* 4, 1–19. doi: 10.1038/s41572-018-0005-8

Billaud, M., Seneca, F., Tambutté, E., and Czerucka, D. (2022). An increase of seawater temperature upregulates the expression of *Vibrio parahaemolyticus* virulence factors implicated in adhesion and biofilm formation. *Front. Microbiol.* 13:840628. doi: 10.3389/fmicb.2022.840628

Bina, X. R., Howard, M. F., Ante, V. M., and Bina, J. E. (2016). *Vibrio cholerae* LeuO links the ToxR regulon to expression of lipid a remodeling genes. *Infect. Immun.* 84, 3161–3171. doi: 10.1128/IAI.00445-16

Boles, B. R., and McCarter, L. L. (2002). Vibrio parahaemolyticus scrABC, a novel operon affecting swarming and capsular polysaccharide regulation. J. Bacteriol. 184, 5946–5954. doi: 10.1128/JB.184.21.5946-5954.2002

Çam, S., and Brinkmeyer, R. (2020). The effects of temperature, pH, and iron on biofilm formation by clinical versus environmental strains of *Vibrio vulnificus*. *Folia Microbiol*. 65, 557–566. doi: 10.1007/s12223-019-00761-9

Chang, J., Zhou, Y., Li, X., Zhang, M., Zhang, Y., Ni, B., et al. (2024). Identification of an LysR family transcriptional regulator that activates motility and flagellar gene expression in *Vibrio parahaemolyticus*. *Lett. Appl. Microbiol*. 77:ovae059. doi: 10.1093/lambio/ovae059

Chen, Y., Dai, J., Morris, J. G. Jr., and Johnson, J. A. (2010). Genetic analysis of the capsule polysaccharide (K antigen) and exopolysaccharide genes in pandemic *Vibrio parahaemolyticus* O3:K6. *BMC Microbiol*. 10:274. doi: 10.1186/1471-2180-10-274

Chen, L., Qiu, Y., Tang, H., Hu, L. F., Yang, W. H., Zhu, X. J., et al. (2018). ToxR is required for biofilm formation and motility of *Vibrio Parahaemolyticus*. *Biomed. Environ. Sci.* 31, 848–850. doi: 10.3967/bes2018.112

Chen, L., Zhang, M., Li, X., Wu, Q., Xue, X., Zhang, T., et al. (2023). AphA directly activates the transcription of polysaccharide biosynthesis gene scvE in *Vibrio parahaemolyticus*. *Gene* 851:146980. doi: 10.1016/j.gene.2022.146980

Chung, C. H., Fen, S. Y., Yu, S. C., and Wong, H. C. (2016). Influence of oxyR on growth, biofilm formation, and mobility of *Vibrio parahaemolyticus*. *Appl. Environ. Microbiol.* 82, 788–796. doi: 10.1128/AEM.02818-15

Enos-Berlage, J. L., Guvener, Z. T., Keenan, C. E., and McCarter, L. L. (2005). Genetic determinants of biofilm development of opaque and translucent *Vibrio parahaemolyticus*. *Mol. Microbiol.* 55, 1160–1182. doi: 10.1111/j.1365-2958.2004.04453.x

Faruque, S. M., Biswas, K., Udden, S. M., Ahmad, Q. S., Sack, D. A., Nair, G. B., et al. (2006). Transmissibility of cholera: in vivo-formed biofilms and their relationship to infectivity and persistence in the environment. *Proc. Natl. Acad. Sci. USA* 103, 6350–6355. doi: 10.1073/pnas.0601277103

Ferreira, R. B., Chodur, D. M., Antunes, L. C., Trimble, M. J., and McCarter, L. L. (2012). Output targets and transcriptional regulation by a cyclic dimeric GMP-responsive circuit in the *Vibrio parahaemolyticus* Scr network. *J. Bacteriol.* 194, 914–924. doi: 10.1128/JB.05807-11

Flemming, H. C., and Wingender, J. (2010). The biofilm matrix. *Nat. Rev. Microbiol.* 8, 623–633. doi: 10.1038/nrmicro2415

Frischkorn, K. R., Stojanovski, A., and Paranjpye, R. (2013). *Vibrio parahaemolyticus* type IV pili mediate interactions with diatom-derived chitin and point to an unexplored mechanism of environmental persistence. *Environ. Microbiol.* 15, 1416–1427. doi: 10.1111/1462-2920.12093

Gao, H., Zhang, Y., Han, Y., Yang, L., Liu, X., Guo, Z., et al. (2011). Phenotypic and transcriptional analysis of the osmotic regulator OmpR in *Yersinia pestis*. *BMC Microbiol*. 11:39. doi: 10.1186/1471-2180-11-39

Gode-Potratz, C. J., Chodur, D. M., and McCarter, L. L. (2010). Calcium and iron regulate swarming and type III secretion in *Vibrio parahaemolyticus*. *J. Bacteriol*. 192, 6025–6038. doi: 10.1128/JB.00654-10

Jenal, U., Reinders, A., and Lori, C. (2017). Cyclic di-GMP: second messenger extraordinaire. *Nat. Rev. Microbiol.* 15, 271–284. doi: 10.1038/nrmicro.2016.190

Kim, Y. K., and McCarter, L. L. (2007). ScrG, a GGDEF-EAL protein, participates in regulating swarming and sticking in *Vibrio parahaemolyticus*. *J. Bacteriol*. 189, 4094–4107. doi: 10.1128/JB.01510-06

Kimbrough, J. H., Cribbs, J. T., and McCarter, L. L. (2020). Homologous c-di-GMP-binding scr transcription factors orchestrate biofilm development in *Vibrio parahaemolyticus*. *J. Bacteriol.* 202:e00723-19. doi: 10.1128/JB.00723-19

Kimbrough, J. H., and McCarter, L. L. (2021). Identification of three new GGDEF and EAL domain-containing proteins participating in the Scr surface colonization regulatory network in *Vibrio parahaemolyticus*. *J. Bacteriol*. 203:e00409-20. doi: 10.1128/JB.00409-20

Lee, K. J., Kim, J. A., Hwang, W., Park, S. J., and Lee, K. H. (2013). Role of capsular polysaccharide (CPS) in biofilm formation and regulation of CPS production by quorum-sensing in *Vibrio vulnificus*. *Mol. Microbiol.* 90, 841–857. doi: 10.1111/mmi.12401

Li, X., Chang, J., Zhang, M., Zhou, Y., Zhang, T., Zhang, Y., et al. (2024). The effect of environmental calcium on gene expression, biofilm formation and virulence of *Vibrio parahaemolyticus*. *Front. Microbiol.* 15:1340429. doi: 10.3389/fmicb.2024.1340429

Li, X., Sun, J., Zhang, M., Xue, X., Wu, Q., Yang, W., et al. (2021). The effect of salinity on biofilm formation and c-di-GMP production in *Vibrio parahaemolyticus*. *Curr. Microbiol.* 79:25. doi: 10.1007/s00284-021-02723-2

Li, X., Zhang, X., Zhang, M., Luo, X., Zhang, T., Liu, X., et al. (2024). Environmental magnesium ion affects global gene expression, motility, biofilm formation and virulence of *Vibrio parahaemolyticus*. *Biofilms* 7:100194. doi: 10.1016/j.biofilm.2024.100194

Liu, M., Nie, H., Luo, X., Yang, S., Chen, H., and Cai, P. (2022). A polysaccharide biosynthesis locus in *Vibrio parahaemolyticus* important for biofilm formation has homologs widely distributed in aquatic Bacteria mainly from Gammaproteobacteria. *mSystems* 7:e0122621. doi: 10.1128/msystems.01226-21

Lu, R., Sun, J., Qiu, Y., Zhang, M., Xue, X., Li, X., et al. (2021). The quorum sensing regulator OpaR is a repressor of polar flagellum genes in *Vibrio parahaemolyticus*. *J. Microbiol. (Seoul, Korea)* 59, 651–657. doi: 10.1007/s12275-021-0629-3

Makino, K., Oshima, K., Kurokawa, K., Yokoyama, K., Uda, T., Tagomori, K., et al. (2003). Genome sequence of *Vibrio parahaemolyticus*: a pathogenic mechanism distinct from that of V cholerae. *Lancet (London, England)* 361, 743–749. doi: 10.1016/S0140-6736(03)12659-1

Martínez-Méndez, R., Camacho-Hernández, D. A., Sulvarán-Guel, E., and Zamorano-Sánchez, D. (2021). A trigger phosphodiesterase modulates the global c-di-GMP Pool, motility, and biofilm formation in *Vibrio parahaemolyticus*. *J. Bacteriol*. 203:e0004621. doi: 10.1128/JB.00046-21

Mayo-Pérez, S., Gama-Martínez, Y., Dávila, S., Rivera, N., and Hernández-Lucas, I. (2023). LysR-type transcriptional regulators: state of the art. *Crit. Rev. Microbiol.* 50, 598–630. doi: 10.1080/1040841X.2023.2247477

Ni, B., Li, W., Chang, J., Zhou, Y., Li, X., Tian, Z., et al. (2024). AcsS negatively regulates the transcription of type VI secretion system 2 genes in *Vibrio parahaemolyticus*. *Curr. Microbiol.* 81:330. doi: 10.1007/s00284-024-03855-x

Ni, B., Tian, Z., Chang, J., Zhou, Y., Li, X., Zhang, M., et al. (2025). Acss inhibits the hemolytic activity and thermostable direct hemolysin (TDH) gene expression in *Vibrio parahaemolyticus*. *Can. J. Microbiol.* 71, 1–6. doi: 10.1139/cjm-2024-0114

Ortet, P., Whitworth, D. E., Santaella, C., Achouak, W., and Barakat, M. (2015). P2CS: updates of the prokaryotic two-component systems database. *Nucleic Acids Res.* 43, D536–D541. doi: 10.1093/nar/gku968

Parales, R. E., and Harwood, C. S. (1993). Construction and use of a new broad-host-range lacZ transcriptional fusion vector, pHRP309, for gram- bacteria. Gene~133, 23-30.~doi: 10.1016/0378-1119(93)90220-W

Pratt, J. T., McDonough, E., and Camilli, A. (2009). PhoB regulates motility, biofilms, and cyclic di-GMP in *Vibrio cholerae*. *J. Bacteriol*. 191, 6632–6642. doi: 10.1128/JB.00708-09

Sharan, M., Vijay, D., Dhaka, P., Bedi, J. S., and Gill, J. P. S. (2022). Biofilms as a microbial hazard in the food industry: a scoping review. *J. Appl. Microbiol.* 133, 2210–2234. doi: 10.1111/jam.15766

- Shime-Hattori, A., Iida, T., Arita, M., Park, K. S., Kodama, T., and Honda, T. (2006). Two type IV pili of *Vibrio parahaemolyticus* play different roles in biofilm formation. *FEMS Microbiol. Lett.* 264, 89–97. doi: 10.1111/j.1574-6968.2006.00438.x
- Sun, F., Zhang, Y., Wang, L., Yan, X., Tan, Y., Guo, Z., et al. (2012). Molecular characterization of direct target genes and cis-acting consensus recognized by quorumsensing regulator AphA in *Vibrio parahaemolyticus*. *PLoS One* 7:e44210. doi: 10.1371/journal.pone.0044210
- Tague, J. G., Regmi, A., Gregory, G. J., and Boyd, E. F. (2021). Fis connects two sensory pathways, quorum sensing and surface sensing, to control motility in *Vibrio parahaemolyticus*. Front. Microbiol. 12:669447. doi: 10.3389/fmicb.2021.669447
- Wu, Q., Li, X., Zhang, M., Xue, X., Zhang, T., Sun, H., et al. (2023). The phase variation between wrinkly and smooth colony phenotype affects the virulence of *Vibrio parahaemolyticus*. *Arch. Microbiol.* 205:382. doi: 10.1007/s00203-023-03719-1
- Wu, X., Zhou, L., Ye, C., Zha, Z., Li, C., Feng, C., et al. (2023). Destruction of self-derived PAMP via T3SS2 effector VopY to subvert PAMP-triggered immunity mediates *Vibrio parahaemolyticus* pathogenicity. *Cell Rep.* 42:113261. doi: 10.1016/j.celrep.2023.113261
- Xue, X. F., Zhnag, M. M., Sun, J. F., Li, X., Wu, Q. M., Yin, Z., et al. (2022). H-NS represses biofilm formation and c-di-GMP synthesis in *Vibrio parahaemolyticus*. *Biomed. Environ. Sci.* 35, 821–829. doi: 10.3967/bes2022.106
- Yang, L., Zhan, L., Han, H., Gao, H., Guo, Z., Qin, C., et al. (2010). The low-salt stimulon in *Vibrio parahaemolyticus*. *Int. J. Food Microbiol*. 137, 49–54. doi: 10.1016/j.ijfoodmicro.2009.11.006
- Yildiz, F. H., and Visick, K. L. (2009). Vibrio biofilms: so much the same yet so different. *Trends Microbiol.* 17, 109–118. doi: 10.1016/j.tim.2008.12.004
- Zhang, M., Cai, L., Luo, X., Li, X., Zhang, T., Wu, F., et al. (2023). Effect of sublethal dose of chloramphenicol on biofilm formation and virulence in *Vibrio parahaemolyticus*. *Front. Microbiol.* 14:1275441. doi: 10.3389/fmicb.2023.1275441
- Zhang, Y., Hu, L., Qiu, Y., Osei-Adjei, G., Tang, H., Zhang, Y., et al. (2019). QsvR integrates into quorum sensing circuit to control *Vibrio parahaemolyticus* virulence. *Environ. Microbiol.* 21, 1054–1067. doi: 10.1111/1462-2920.14524

- Zhang, Y., Liu, H., Gu, D., Lu, X., Zhou, X., and Xia, X. (2020). Transcriptomic analysis of PhoR reveals its role in regulation of swarming motility and T3SS expression in *Vibrio parahaemolyticus*. *Microbiol. Res.* 235:126448. doi: 10.1016/j.micres.2020.126448
- Zhang, M., Luo, X., Li, X., Zhang, T., Wu, F., Li, M., et al. (2023). L-arabinose affects the growth, biofilm formation, motility, c-di-GMP metabolism, and global gene expression of *Vibrio parahaemolyticus. J. Bacteriol.* 205:e0010023. doi: 10.1128/jb.00100-23
- Zhang, Y., Qiu, Y., Gao, H., Sun, J., Li, X., Zhang, M., et al. (2021). OpaR controls the metabolism of c-di-GMP in *Vibrio parahaemolyticus*. *Front. Microbiol.* 12:676436. doi: 10.3389/fmicb.2021.676436
- Zhang, L., Weng, Y., Wu, Y., Wang, X., Yin, Z., Yang, H., et al. (2018). H-NS is an activator of exopolysaccharide biosynthesis genes transcription in *Vibrio parahaemolyticus*. *Microb. Pathog.* 116, 164–167. doi: 10.1016/j.micpath.2018.01.025
- Zhang, M., Xue, X., Li, X., Wu, Q., Zhang, T., Yang, W., et al. (2023). QsvR and OpaR coordinately repress biofilm formation by *Vibrio parahaemolyticus*. *Front. Microbiol.* 14:1079653. doi: 10.3389/fmicb.2023.1079653
- Zhang, Y., Xue, X., Sun, F., Li, X., Zhang, M., Wu, Q., et al. (2023). Quorum sensing and QsvR tightly control the transcription of vpa0607 encoding an active RNase II-type protein in *Vibrio parahaemolyticus*. *Front. Microbiol.* 14:1123524. doi: 10.3389/fmicb.2023.1123524
- Zhang, M., Xue, X., Sun, J., Wu, Q., Li, X., Zhou, D., et al. (2022). ToxR represses the synthesis of c-di-GMP in *Vibrio parahaemolyticus*. *Sheng Wu Gong Cheng Xue Bao* 38, 4719–4730. doi: 10.13345/j.cjb.210790
- Zhang, Y., Zhang, Y., Gao, H., Zhang, L., Yin, Z., Huang, X., et al. (2017). *Vibrio parahaemolyticus* CalR down regulates the thermostable direct hemolysin (TDH) gene transcription and thereby inhibits hemolytic activity. *Gene* 613, 39–44. doi: 10.1016/j.gene.2017.03.001
- Zhang, Y., Zhang, T., Qiu, Y., Zhang, M., Lu, X., Yang, W., et al. (2023). Transcriptomic profiles of *Vibrio parahaemolyticus* during biofilm formation. *Curr. Microbiol.* 80:371. doi: 10.1007/s00284-023-03425-7
- Zhong, X., Lu, Z., Wang, F., Yao, N., Shi, M., and Yang, M. (2022). Characterization of GefA, a GGEEF domain-containing protein that modulates *Vibrio parahaemolyticus* motility, biofilm formation, and virulence. *Appl. Environ. Microbiol.* 88:e0223921. doi: 10.1128/aem.02239-21